The Crystal Structure and Physicochemical Characteristics of 2-Hydroxy-N-[3(5)-pyrazolyl]-1,4-naphthoquinone-4-imine, a New Antitrypanosomal Compound

Submitted: February 2, 2005; Accepted: September 14, 2005; Published: December 27, 2005

Norma R. Sperandeo,[1] Alicia Karlsson,[2] Silvia Cuffini,[3] Silvina Pagola,[4] and Peter W. Stephens[4]

[1]Departamento de Farmacia, Facultad de Ciencias Químicas, Universidad Nacional de Córdoba, 5000- Córdoba, Argentina
[2]Cátedra de Métodos de Investigación de Minerales, Facultad Ciencias Exactas, Físicas y Naturales, Universidad Nacional de Córdoba, Córdoba, Argentina
[3]Agencia Córdoba Ciencia, CEPROCOR, Córdoba, Argentina
[4]Department of Physics and Astronomy, SUNY at Stony Brook, Stony Brook, NY 11974-3800

ABSTRACT

This study was designed to investigate the physical characteristics and crystalline structure of 2-hydroxy-*N*-[3(5)-pyrazolyl]-1,4-naphthoquinone-4-imine (PNQ), a new active compound against *Trypanosoma cruzi*, the causative agent of American trypanosomiasis. Methods used included differential scanning calorimetry, thermogravimetry, hot stage microscopy, polarized light microscopy (PLM), Fourier-transform infrared (FTIR) spectroscopy, and high-resolution X-ray powder diffraction (HR-XRPD). According to PLM and HR-XRPD data, PNQ crystallized as red oolitic crystals (absolute methanol) or prisms (dimethyl sulfoxide [DMSO]-water) with the same internal structure. The findings obtained with HR-XRPD data (applying molecular location methods) showed a monoclinic unit cell [a = 18.4437(1) Å, b = 3.9968(2) Å, c = 14.5304(1) Å, α = 90°, β = 102.71(6)°, γ = 90°, V = 1044.9(1) Å^3, Z = 4, space group $P2_1/c$], and a crystal structure (excluding H-positions) described by parallel layers in the direction of the *b*-axis, with molecules held by homochemical (phenyl-phenyl and pyrazole-pyrazole) van der Waals interactions. In addition, FTIR spectra displayed the NH-pyrazole stretch overlapped with the OH absorption at 3222 cm^{-1}, typical of -NH and -OH groups associated through H-bondings; and a carbonyl stretching absorption at 1694 cm^{-1}, indicating a non-extensively H-bonded quinonic C=O, which was in accordance with the solved crystal structure of PNQ. The existence of such cohesive forces shed light on the thermoanalytical data, which revealed that PNQ is a stable solid, unaffected by oxygen that decomposed without melting above 260°C.

KEYWORDS: anti-Trypanosoma cruzi agent, high-resolution X-ray powder diffraction, crystal structure, differential scanning calorimetry.

Corresponding Author: Norma R. Sperandeo, Departamento de Farmacia, Facultad de Ciencias Químicas, Universidad Nacional de Córdoba, 5000-Córdoba, Argentina. Tel: +54-351-4334163; Fax: +54-351-4334127; E-mail: nrscor@dqo.fcq.unc.edu.ar

INTRODUCTION

The need for new active drugs against *Trypanosoma cruzi,* the etiological agent of American Trypanosomiasis (Chagas disease), is widely recognized. Currently, there are between 16 and 18 million chronically infected carriers of Chagas´ disease in the tropics and subtropics of North and South America, and more than 100 million people at risk.[1] However, at present there are only 2 drugs available, benznidazole and nifurtimox, which although very helpful when given during the acute stage of infection, are ineffective in the chronic period and produce adverse side effects due to their toxicity.[2] In addition, the growth of parasite resistance against the 2 mentioned chemotherapeutic drugs cannot be ignored, emphasizing the importance of the search for new anti-*T. cruzi* agents.

Naphthoquinone-based agents form a large class of therapeutically significant drugs, ranging from antimicrobials[3] to antineoplastics.[4] Our interest in quinone chemistry prompted us to give special attention to the synthesis and biological properties of pyrazolylnaphthoquinones, a new class of naphthoquinone derivatives, finding that 2-Hydroxy-*N*-[3(5)-pyrazolyl]-1,4-naphthoquinone-4-imine (PNQ) exhibits promising activity against *T. cruzi*.[5]

At present, the study of the solid state properties of new substances is essential for the development and approval of novel drug compounds[6] mostly because of the importance of the physical properties of the solid state in the bioavailability of drugs administered in the solid state as part of a solid dosage form. In fact, in recent years, efforts have been directed to elucidate the physicochemical properties of active pharmaceutical ingredients (APIs)[7,8]; specifically, knowledge of the 3-dimensional structure of APIs has aided in the understanding of their solid state chemistry and pharmaceutical properties. With these aims in mind, a study of the solid state of PNQ was undertaken since its physical properties and crystalline structure have not yet been studied. Thus, in this study 2 samples of PNQ prepared by recrystallization from absolute methanol (PNQ-M) and dimethyl sulfoxide (DMSO)-water 5:1 (PNQ-D) are described and characterized by means of differential scanning

calorimetry (DSC), thermogravimetry (TG), Fourier-transform infrared spectroscopy (FTIR), high-resolution X-ray powder diffraction (HR-XRPD), hot stage microscopy (HSM), and polarized light microscopy (PLM). Also, the crystal structure of PNQ was solved using molecular location methods applied to HR-XRPD.[9,10]

Materials and Methods

Materials

PNQ was synthesized according to our previously reported method.[5] Crystallization assays from solvents of different polarities were performed in order to identify the most adequate crystallization conditions, finding that PNQ crystallized with good yields only in absolute methanol and DMSO-water (5:1). The recrystallization procedure was as follows: A hot saturated solution of drug in absolute methanol or DMSO-water was filtered and allowed to reach room temperature (RT). Next, it was cooled at –20ºC for 2 days. The formed crystals were filtered and dried in vacuo. The purity of the crystals was checked by thin-layer chromatography (TLC) and paper electrophoresis, finding that they were chromatographically and electrophoretically homogeneous; the crystals were also examined by high-resolution mass spectra (performed at the McMaster Center for Mass Spectrometry, Hamilton, Ontario, Canada). For TLC analyses, precoated plates of silica gel 60 F_{254} (Merck, Whitehouse Station, NJ) were used. Spots were visualized with UV and daylight. Solvents of analytical reagent grade and distilled water were employed. All the studies were performed without grinding the crystals, except for FTIR and HR-XRPD analyses.

Methods

The DSC and TG measurements were recorded on MDSC 2920 and TG 2950 analyzers (TA Instruments Inc, New Castle, DE), respectively. The operating conditions for both instruments (open pan system) were as follows: heating rate, 10 deg.min^{-1}; atmosphere, static air or dynamic N_2 (99.99%, flow rate 50 mL/min). The DSC and TG temperature axes were calibrated with indium (99.99%; melting point, 156.60°C) and by the Curie point of Ni (353°C), respectively. Empty aluminum pans were used as references and samples of ~2 mg were used. The reported DSC values were the average of at least 2 independent measurements. Data were treated with Thermal Solutions software (TA Instruments).

The physical and morphological changes of the samples that occurred during the process of heating were observed through a microscope fitted with a Kofler hot-stage (Leitz, Wetzlar, Germany) at a constant rate from RT (~ 8ºC/min) up to 280ºC. In order to provide experimental conditions similar to those in air, the samples were not embedded in silicone oil.[11] In addition, the crystallinity of the samples was assessed by measuring their birefringence according to the *United States Pharmacopeia (USP)* test of crystallinity[12] (ie, the solid was suspended in silicone immersion oil and examined under a polarized light microscope equipped with crossed polarizers [petrographic microscope]).

HR-XRPD data were collected at RT at the SUNY X3B1 beamline, National Synchrotron Light Source (Brookhaven National Laboratory, Upton, NY). The samples were chopped in order to reduce the size of the crystals; then they were sealed in thin-walled glass capillaries and spun, while collecting data. A Si (111) double-crystal monochromator (calibrated using a National Institute of Standards and Technology (NIST) standard Al_2O_3 plate) was used. The incident radiation intensity was monitored with an ion chamber and the diffracted intensity was measured with an NaI (Tl) scintillation detector. The horizontal and vertical resolutions of the diffractometer were given by slits and by a Ge (111) analyzer crystal, respectively. The crystal structure solution procedure is summarized as follows: The 2θ positions of the first 20 peaks were determined using GUFI,[13] a program for visualizing and processing powder diffraction patterns, estimating background intensities, fitting peaks, indexing, etc. In order to obtain the unit cell parameters, the angular positions of the peaks were entered into the program ITO[14] using the zone-indexing method. After that, the Le Bail algorithm was employed to calculate the diffraction pattern and to minimize the difference between observed and calculated diffraction intensities without a crystallographic model (the unknown atomic positions). A selected profile function was used both to simulate the various diffraction peaks as to refine profile shape, asymmetry and unit cell parameters, and background intensity, while the scale factor was not varied. In this manner, the correctness of the calculated unit cell parameters was checked by a Le Bail fit[15] using the program FULLPROF.[16] The systematic absences (Bragg reflections that are allowed by symmetry but with null intensities) were analyzed to determine the space group. In order to compare the final agreement factor values (R_{wp}) with and without the inclusion of the crystallographic model, another Le Bail fit was done with the program GSAS.[17] This fit produced a set of integrated intensities of the Bragg reflections, of which the first 50 were used to obtain a set of atomic positions by location of the molecules in the unit cell. The molecular location step (structure solution) was done with the program PSSP.[18] Within this structure solution method, the simulated annealing algorithm was used to find an optimum set of parameters (molecular positions in the unit cell as well as the Eulerian and torsional angles that defined the molecular orientations and

conformations, respectively). This treatment produced the best agreement between the experimental (Le Bail) and trial model integrated intensities of the reflections, among a large number of trial structures postulated at decreasing values of the temperature parameter. The geometries of the molecular fragments known to be present in the unit cell are described with a set of Cartesian coordinates. In this case, the PNQ molecule was modeled adapting 2 fragments (from 2-amino-1,4-naphthoquinone-4-iminium chloride dihydrate and 3-nitropyrazole) taken from the Cambridge Structural Database (CSD) entries ANPQIM and RIKNOO, respectively.[19] The analysis of the cell volume and possible densities allowed to estimate Z (the number of molecules per unit cell). The wavelength, unit cell parameters, space group symmetry operations, Cartesian coordinates, and total number of atoms per unit cell were entered into the program PSSP.[18] During the simulated annealing runs, the molecular fragments were not attached but rather searched independently through the 12-dimensional space positions and orientations of the 2 fragments (3 unit cell positions and 3 Eulerian angles for each fragment). The annealing schedule used an initial temperature factor of 50, a temperature decrement factor of 0.8, a final temperature factor of 0.001 and 5000 cycles. Several simulated annealing runs were performed.

In order to corroborate that the fragments searched gave rise to the PNQ molecule, and also to check the intermolecular interactions found, the structure solution with the lowest value of the agreement factor "*S*" was visualized using the program Ortep-3 for Windows.[20] The obtained atomic positions were refined using the Rietveld method implemented in the program GSAS,[17] through which the difference between calculated and experimental diffraction intensities is minimized using a multi-variable least-squares algorithm. The unit cell positions and Eulerian angles of the molecular fragments (determined with the program PSSP) were entered into the program GSAS to generate an initial set of atomic positions. Last, the Rietveld method was used to obtain the ultimate set of refined atomic positions and other crystallographic parameters, such as thermal and occupancy factors. All the software to process the HR-XRPD data were run under the Windows operating system. The Internet addresses used to download these programs are included in the References section.

FTIR spectra were recorded on a Nicolet 5-SXC FTIR spectrophotometer (Nicolet Instruments Corp, Madison, WI). Samples were prepared as KBr pellets (~1 mg in 200 mg of KBr) with a mini-press (Hidráulicos Delfabro, Córdoba, Argentina) at 6 tons without any extra grinding. The spectra were collected with 40 scans, at 8 cm^{-1} resolution, and processed with the Nicolet OMNIC 1.1 program (Nicolet).

Results and Discussion

Solid Phases and HR-XRPD

Microscopic examination with polarized light revealed that PNQ is a red crystalline substance that crystallized in at least 2 different crystalline habits. Indeed, PNQ crystallized from absolute methanol (PNQ-M) as spherical or nearly rounded crystals (radiated from a center producing red oolitic forms) whose radii were of ~1 mm. Conversely, PNQ-D consisted of long red planar fibers (~300 μm) with birefringence (0.20) and straight extinction when examined under polarized light. The fibers were pleochroic from yellow to orange, and the average refractive index measured was 1.55. The optic plane was parallel to the fiber axis.

The HR-PDRX diffractograms of PNQ-M and PNQ-D are depicted in Figure 1. As can be seen, the patterns of both samples showed the same peaks, indicating that they have the same internal structure. Indeed, the diffraction data were indexed to the same reduced monoclinic unit cell [PNQ-M: a = 18.436 Å, b = 3.997 Å, c = 14.529 Å, α= 90°, β = 102.697°, γ = 90°, cell volume = 1044 Å3 with M (20) = 52.6; and PNQ-D: a = 18.430 Å, b = 3.999 Å, c = 14.523 Å, α = 90°, β = 102.750°, γ = 90°, cell volume = 1044 Å3 with M(20) = 89]. In order to solve the crystal structure of PNQ, the HR-XRPD pattern was further analyzed as described in the Methods section. On the basis of results of a Le Bail fit done in the lowest symmetry monoclinic space group (P2) and from the observation of the systematic absences, the space group $P2_1/c$ was determined. The R_{wp} obtained in the Le Bail fit (GSAS program) was 7.26%. Thus, from the molecular weight and the calculated cell volume, Z = 4 was suggested as it gave rise to a reasonable density value (1.5 g/cm^3).

For the crystal structure solution, we hypothesized that there was one molecule (illustrated in the inset of Figure 1) in the general position of the space group $P2_1/c$. The PNQ molecule was modeled adapting 2 fragments from 2-amino-1,4-naphthoquinone-4-iminium chloride dihydrate and 3-nitropyrazole.[19] These fragments were not attached but rather searched through the 12-dimensional space of position and orientation of the 2 fragments.

The program PSSP obtained a plausible solution (agreement factor S = 0.029) that located both molecular fragments independently within the unit cell forming the PNQ molecules. In the final Rietveld refinement (Figure 2), there were no restraints on the bond between the iminic nitrogen and the pyrazole ring (Figure 1 inset), which refined to 1.39(4) Å; the bond angles also had reasonable values: C4—N4—C3′ 128(4)º, N4—C3′—N2′ 115(7)º, and N4—C3′—C4′ 131(7)º (Table 1). The adopted molecular conformation was not flat and the torsion angle (C4—N4—C3′

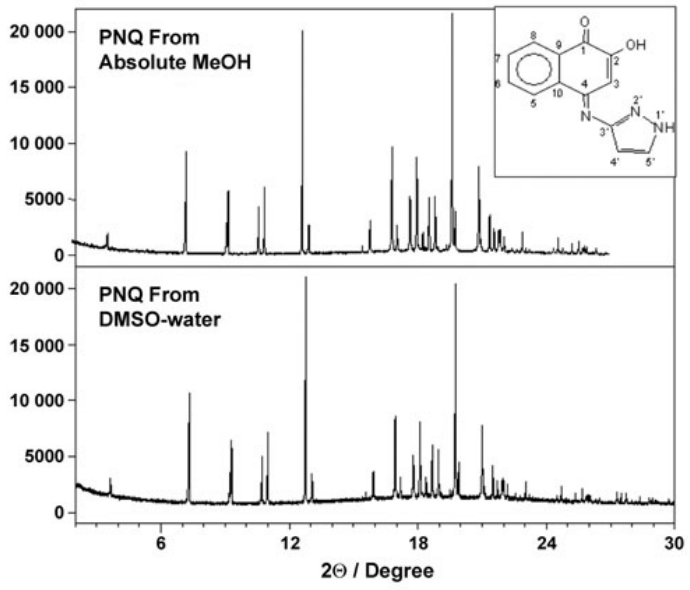

Figure 1. HR-XRPD patterns of PNQ recrsytallized from absolute methanol (PNQ-M) and DMSO-water (PNQ-D). Inset: chemical structure of PNQ and atomic numbering used in this study.

—N2′) between the 2 rings was −47(9) degrees. The agreement factors obtained in the refinement were R_{wp} = 7.52%, R_I = 8.49%, and χ^2 = 2.96, with the following refined cell parameters: a = 18.4437(1) Å, b = 3.99677(2) Å, c = 14.5304 (1) Å, α = 90°, β = 102.7086(6)°, γ = 90°, and cell volume = 1044.88(1) Å^3. The atomic positions, thermal and occupancy factors are shown in Table 2. The standard deviations informed by the program GSAS were corrected following a widely used procedure.[21]

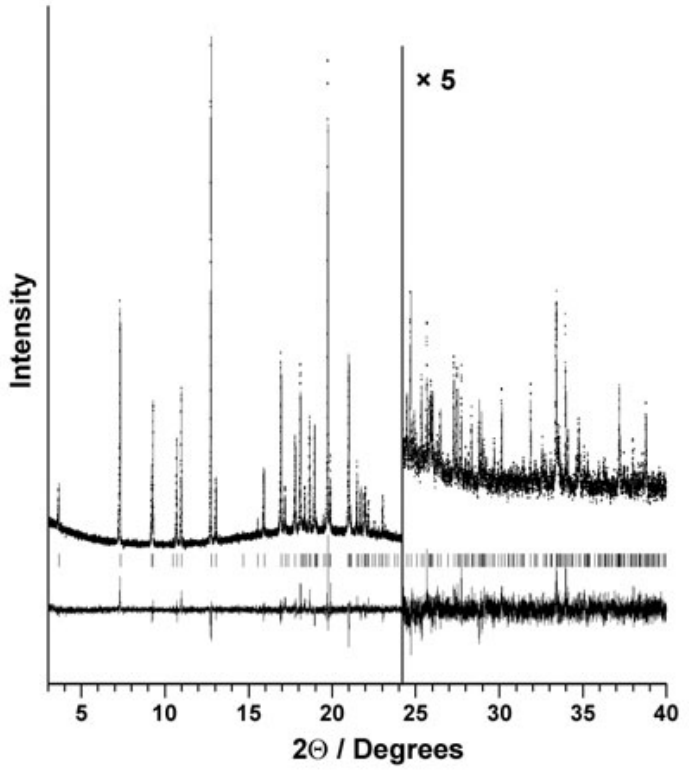

Figure 2. Rietveld refinement of the HR-XRPD pattern of PNQ. Experimental data (dots), calculated pattern (solid line), and difference curve (at the bottom).

The crystal structure of PNQ is shown in Figure 3 along the [010] direction, which indicates that the spatial arrangement of the molecules can be described as parallel layers in

Table 1. Selected Bond Lengths (in Å) and Bond Angles (in degrees)*

Atoms	Bond Distance	Atoms	Bond Angle
O1-C1′	1.22(4)	C4-N4-C3′	128(4)
C5-C10	1.39(2)	N4-C4-C10	119(2)
O2-C2	1.32(4)	N1’-N2’-C3′	104(5)
C1-C2	1.51(3)	C10-C4-C3	121.5(19)
N4-C4	1.33(3)	C2-C3-C4	121.5(19)
C10-C4	1.48(3)	N2’-N1’-H1’	118(10)
N4-C3′	1.39(4)	C3′- C4’-C5′	103(4)
C2-C3	1.38(3)	C5′-N1’-H1’	129(11)
N1’-N2’	1.32(12)	N4-C3′-N2’	115(7)
C3-C4	1.40(4)	C8-C7-C6	120.0(19)
N2’-C3′	1.31(10)	N4-C3′-C4’	131(7)
C3′-C4’	1.37(10)	C7-C8-C9	120(2)
N1’-C5′	1.33(10)	N2’-C3′-C4’	114(6)
C4’-C5′	1.36(13)	C7-C6-C5	120(2)
N1’-H1’	0.77(12)	N1’-C5′-C4’	108(6)
C7-H7	1.05(3)	C1-C9-C10	121(7)
C6-C7	1.39(4)	C8-C7-H7	125(3)
C8-H8	0.92(4)	C8-C9-C1	120(5)
C7-C8	1.38(4)	C6-C7-H7	115(3)
C6-H6	0.97(4)	C8-C9-C10	120(3)
C8-C9	1.39(10)	C7-C8-H8	122(2)
C5-H5	1.09(4)	C6-C5-C10	121.0(18)
C6-C5	1.37(3)	C9-C8-H8	117(3)
C3-H3	0.96(3)	C9-C1-C2	118(4)
C9-C1	1.46(3)	C7-C6-H6	117(3)
C4’-H4’	0.95(6)	O1-C1-C9	123(4)
C9-C10	1.41(7)	C5-C6-H6	123(3)
C5′-H5′	0.98(14)	O1-C1-C2	119(2)
		C6-C5-H5	116(3)
		C5-C10-C4	122.7(17)
		C10-C5-H5	123(3)
		C9-C10-C4	118(3)
		C2-C3-H3	118(4)
		C9-C10-C5	119(3)
		C4-C3-H3	120(3)
		O2-C2-C3	125(2)
		C3′-C4’-H4’	136(15)
		O2-C2-C1	115(2)
		C5′-C4’-H4’	121(14)
		C1-C2-C3	120(2)
		N1’-C5′-H5′	122(11)
		N4-C4-C3	119(2)
		C4’-C5′-H5′	130(10)

* ESDs (Estimated Standard Deviations) are shown in parentheses.

Table 2. Atomic Positions, Thermal and Occupancy Factors for PNQ After the Rietveld Refinement*

Atom	X	Y	Z	Ui/Ue*100	Occupancy
C1	0.685(1)	0.3376(6)	0.572(2)	0.025(10)	1
C2	0.758(1)	0.157(6)	0.581(2)	0.025(10)	1
C3	0.7934(8)	0.158(6)	0.507(2)	0.025(10)	1
C4	0.7637(9)	0.326(7)	0.423(2)	0.025(10)	1
C5	0.658(1)	0.652(7)	0.323(1)	0.025(10)	1
C6	0.590(1)	0.802(6)	0.311(2)	0.025(10)	1
C7	0.552(1)	0.800(6)	0.384(2)	0.025(10)	1
C8	0.5838(8)	0.654(5)	0.469(2)	0.025(10)	1
C9	0.653(6)	0.501(4)	0.482(1)	0.025(10)	1
C10	0.6910(9)	0.500(5)	0.408(1)	0.025(10)	1
C3′	0.875(1)	0.24(2)	0.359(6)	0.025(10)	1
C4’	0.907(6)	0.05(1)	0.300(2)	0.025(10)	1
C5′	0.981(4)	0.08(1)	0.339(6)	0.025(10)	1
N4	0.801(1)	0.326(9)	0.354(2)	0.025(10)	1
N1’	0.988(3)	0.27(2)	0.416(4)	0.025(10)	1
N2’	0.923(6)	0.37(1)	0.430(4)	0.025(10)	1
O1	0.654(1)	0.330(6)	0.638(2)	0.025(10)	1
O2	0.783(1)	0.007(6)	0.663(2)	0.025(10)	1.05(4)
H3	0.837(1)	0.024(8)	0.512(3)	0.22(18)	1
H5	0.682(2)	0.643(9)	0.261(2)	0.22(18)	1
H6	0.567(2)	0.923(8)	0.254(2)	0.22(18)	1
H7	0.500(1)	0.918(7)	0.369(2)	0.22(18)	1
H8	0.562(1)	0.662(6)	0.520(2)	0.22(18)	1
H1’	1.023(5)	0.31(3)	0.454(7)	0.22(18)	1
H4’	0.89(1)	-0.06(2)	0.241(3)	0.22(18)	1
H5′	1.024(7)	-0.02(2)	0.32(1)	0.22(18)	1

*PNQ indicates 2-hydroxy-*N*-[3(5)-pyrazolyl]-1,4-naphthoquinone-4-imine values corrected per Scott.[21]

the direction of the *b*-axis with molecules held by homochemical (phenyl-phenyl and pyrazole-pyrazole) van der Waals interactions and separated by 3.997 Å. It should be noted that from this powder diffraction experiment, the locations of hydrogens are not determined. In spite of this, H-positions were included in the Rietveld refinement as they came in the original Cambridge Structural Database (CSD) geometries, except from the position of the hydroxyl hydrogen, for which the occupancy factor of the oxygen was instead refined. Considering the nonhydrogen interatomic distances, there is likely to be a H-bond between the hydroxyl hydrogen and the iminic nitrogen of another molecule in the same molecular layer (O$^{\cdots}$N distance of 2.81 Å), approximately along the direction of the c-axis. Furthermore, between the molecules related by the 2_1 axis (in adjacent layers) there would be 2 intermolecular H-bonds (N—H$^{\cdots}$N) linking the pyrazole rings, with distances N$^{\cdots}$N and H$^{\cdots}$N of 2.86 Å and 2.17 Å, respectively. It is interesting to note that in other pyrazole derivatives,[22] similar intermolecular interactions (formation of dimers) have been previously reported.

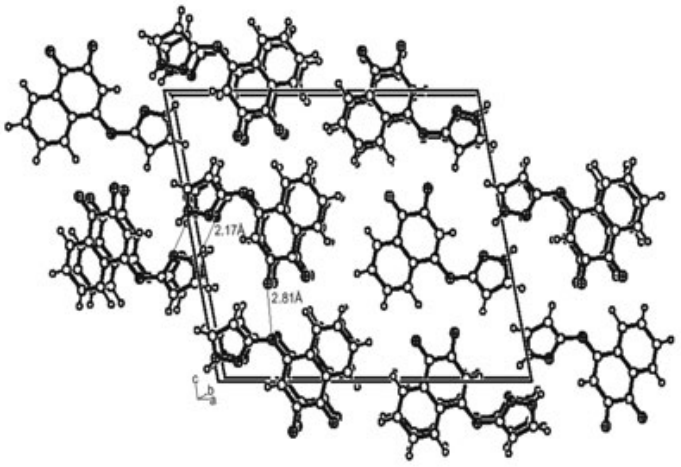

Figure 3. The crystal structure of PNQ (view from the [010] direction).

Fourier-transform Infrared Spectroscopy, Differential Scanning Calorimetry, Thermogravimetry, and Hot Stage Microscopy

FTIR spectra of PNQ-M and PNQ-D (Figure 4) are virtually identical, providing not only additional evidence that the 2 samples had the same crystal lattices and geometries, but also giving some information regarding the intermolecular interactions within the crystals. In particular, the spectra exhibited no bands in the region of free OH or NH, indicating the existence of associated molecules in the lattice.

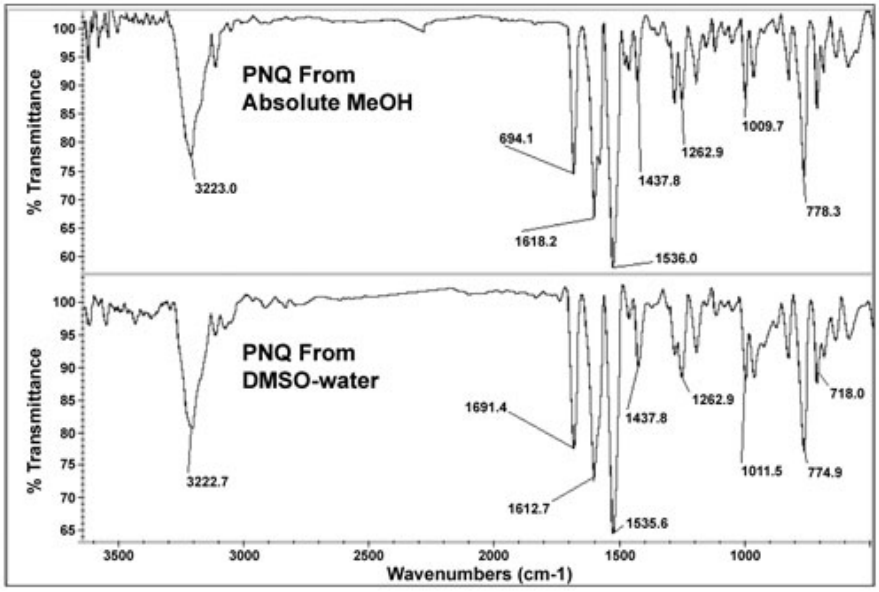

Figure 4. Stacked FTIR spectra (KBr) of PNQ recrystallized from absolute methanol (PNQ-M) and DMSO-water 5:1(PNQ-D).

Indeed, the NH-pyrazole and OH stretch vibrations overlapped, appearing as a broad band centered at 3223 cm^{-1}. The absence of a separated OH absorption can be explained considering that in 2-hydroxy-isoxazolylnapthoquinones,[23,24] the OH band appeared at ~3200 cm^{-1}, the normal position of OH groups associated through H bondings. Thus, the OH group of PNQ-M and PNQ-D is also engaged in H bondings, which caused that it overlapped the normal absorption of the νNH of pyrazole,[25] and this is consistent with the HR-XRPD crystal structure solution of PNQ. Furthermore, the CO stretch of the carbonyl in the naphthoquinone was observed at 1694 cm^{-1}, suggesting that in PNQ the group is less H-bonded than in other hydroxynaphthoquinones, which showed CO absorption bands at ~1670 cm^{-1}, the typical wavenumber for conjugated CO groups. Consistently, the crystal structure solution of PNQ gave the C=O group free of H bondings.

The thermal behavior of PNQ-M and PNQ-D was assessed by DSC, TG-derivative thermogravimetry (DTG), and HSM, and DSC thermal parameters (t_{onset}, t_{max} and heats of transitions [ΔH]) are listed in Table 3.

According to the thermoanalytical data, the samples were solvent-free solids that showed similar thermal behaviors. Indeed, neither DSC desolvation peaks nor TG weight losses were observed below 200ºC. As is exemplified in the case of PNQ-M, the DSC curve in flowing N_2 (Figure 5, upper traces) displayed a single endothermic peak at 264.4ºC, superimposed with an exothermic peak centered at 270.2ºC, suggesting a melting with decomposition process. PNQ-M (and also PNQ-D sample) was visually examined by HSM to assist in the interpretation of the DSC events. Microscopic observations revealed that from RT up to 220ºC, phase modifications and evaporation losses were not produced, which is consistent with the DSC and TG-DTG results. The material began to reduce itself in size at ~230ºC and concurrently, a few transparent orange prisms of PNQ (TLC identification using benzene-ethyl acetate-MeOH-ammonium hydroxide 2:3:1:0:2 as mobile phase) were observed on the cover, typical of a sublimation process. It should be noted that the TG-DTG curves also indicated that the weight loss started before the DSC endothermic peak (Figure 5). On further heating (at ~260ºC), the crystals of the cover started to sublime, while

Table 3. Crystallization Conditions and DSC Data on the Thermal Behavior of PNQ Sample*

Sample	Recrystallization Solvent Temperature/°C	DSC/°C Onset	Peak	Peak	ΔH/J.g^{-1}	Weight/mg†
PNQ-M	MeOH / 62	257.1	264.6‡	270.2 exo	69.7	1.430
PNQ-M	"	257.1	264.8§	271.2 "	68.5	1.284
PNQ-D	DMSO-H_2O/ 100	266.6	271.1§	278.5 "	69.5	1.745

*DSC indicates differential scanning calorimetry; and PNQ, 2-hydroxy-*N*-[3(5)-pyrazolyl]-1,4-naphthoquinone-4-imine.

†Molecular weight: 239.0695.

‡: In flowing N_2 (50 mL.min^{-1}).

§: In static air.

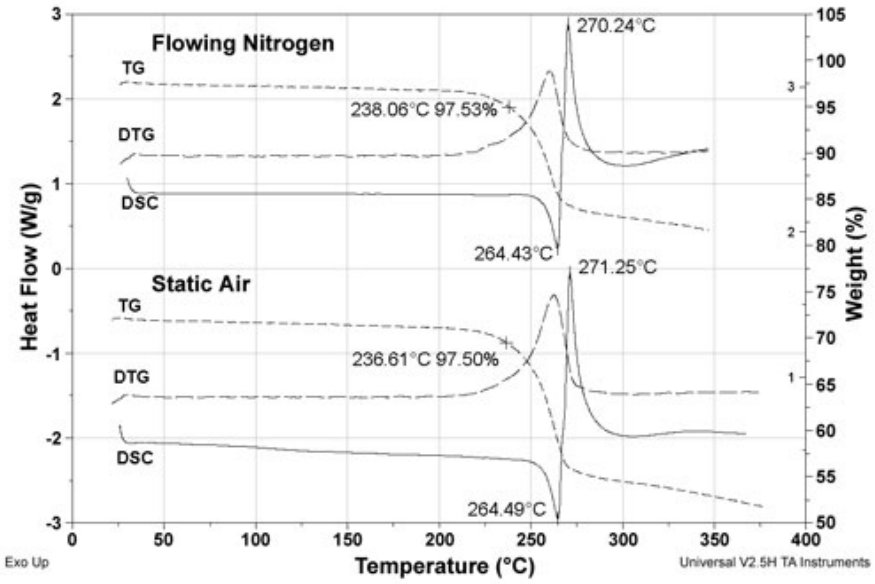

Figure 5. DSC and TG-DTG curves (heating rate of 10°C.min^{-1}) of PNQ from absolute methanol (PNQ-M) performed under flowing N_2 (50 mL.min^{-1}, upper traces) and static air (lower traces).

the crystals on the slide darkened and reduced in size. Finally, at ~280ºC no crystals were observed on the cover, while in the slide, a black solid residue remained. Melted droplets in the slide or in the cover were not discerned. These results shed light on the DSC profile, indicating that the peak at 264ºC could not be ascribed to fusion, thus PNQ is a solid that decomposed without melting.[26]

In order to confirm the conclusions drawn from the Kofler, the DSC and TG curves were also run in static air. As it can be seen in Figure 5 (lower traces), the DSC and TG profiles and also the thermal parameters did not change (Table 3). It should be noted that in no case (flowing N_2 or static air) could the DSC profiles be repeated in a second heating run. These findings demonstrated that the decomposition process experimented by PNQ was not catalyzed by the oxygen of air, indicating not only the validity of the Kofler observations but also providing information about the thermal-oxidative stability of PNQ crystals. In fact, it is known that DSC provided valuable aid in assessing such stability, since the higher the extrapolated onset (t_{onset}) and peak maximum temperature (t_{max}) the more the thermal-oxidative stability of a sample.[27] Hence, the thermal parameters obtained in air (an oxidizing atmosphere) can be used as primary parameters of the resistance of PNQ crystals to thermal-oxidative decomposition. PNQ crystals have high t_{onset} (>250ºC), indicating that the compound is stable as solid at high temperatures and also that it was unaffected by oxygen. Then, PNQ can be safely manipulated in air at RT and even at higher temperatures. Consistently, PNQ-M and PNQ-D crystals stored more than 6 months at RT did not present decomposition products as judged by TLC and DSC analyses.

Regarding PNQ-D, a small difference in its DSC transition temperatures in relation to PNQ-M (Table 3) was seen. This fact does not reflect a difference between the samples at a molecular level (see XRPD and FTIR evidence), but it is likely owing to the differences in crystal habits and particle sizes. In fact, it is known[28,29] that both factors influenced the DSC onset and peak values (ie, less developed crystals), for example needles, are less stable to thermal changes and give endothermic peaks at lower temperatures than more developed crystals such as prisms, which are more stable and give endothermic peaks at higher temperatures.[29] In addition, thermal differences between crystalline samples of the same compound indicated that the energy needed to initiate a chemical or a thermal process varies despite the fact that the energy involved in the process itself remains the same,[30,31] as with PNQ-M and PNQ-D that had similar heats of transition (ΔH, Table 3).

The different morphology of PNQ crystals may also have an effect on their performance. It is known that the performance of a drug can be dependent on the external structure of the crystals, since habits may exert a dominant influence on several pharmaceutical characteristics, among others, suspension syringeability, tableting behavior, and bulk density of the drug.[6,32] For example, a suspension of plate-shaped crystals may be injected with greater ease than one with needle-shaped crystals. Moreover, having the same internal structure, one crystal habit of an active ingredient may tablet well, while another may cause trouble.[32] Furthermore, as it was demonstrated in the case of trimethroprim[33] and diflunisal,[34] habits can also influence the dissolution rates; however, the morphology of the crystals did not alter the pharmacokinetic parameters, since

both drugs were rapidly absorbed. Therefore, it seems that the selection of the proper crystal habit of a drug may be advantageous from a processability point of view, but for rapidly absorbable drugs such an approach will not adversely affect the pharmacokinetic profile.[34]

In the case of PNQ, although systematic solubility and absorption studies have not been performed, we observed that PNQ-M and PNQ-M show poor solubility in water, having a calculated log P (ClogP) similar to that of metoprolol, a high permeable compound with no absorption problems.[35] In this sense, it is noteworthy that in vitro PNQ-M and PNQ-D solutions showed virtually identical anti-*T. cruzi* activity (the IC_{50} values for PNQ-M and PNQ-D were 3.3 $\mu g.mL^{-1}$ and 3.2 $\mu g.mL^{-1}$, respectively) (R Brun, email communication, October 2000) as was expected owing to the insignificant intercrystalline variation in ΔH of transitions (Table 3). Hence, PNQ could be expected to be a rapidly absorbable drug for which its different crystal habits do not influence its absorption. However, this assumption needs to be validated. Thus, studies are planned to evaluate the biopharmaceutical relevance of the crystalline habits of PNQ.

CONCLUSION

The data reported in this article provided a meaningful set of solid-state characteristics of PNQ, ensuring their quality and lot-to-lot reproducibility. It was determined that PNQ can crystallize as red oolits or prisms, having the same crystalline monoclinic unit cell. The crystal structure of PNQ (excluding hydrogen positions) was successfully solved by molecular location methods applied to HR-XRPD data, which indicated that the spatial arrangement of the PNQ molecules consisted in parallel layers in the direction of the b-axis. In addition, it was determined that PNQ crystals exhibit a high thermal-oxidative stability, attributable to the predominance of intermolecular interactions (van der Waals and hydrogen bondings). Consequently, it is not likely to be necessary to protect it from oxygen at RT and even at higher temperatures.

ACKNOWLEDGMENTS

The authors thank SECyT-UNC and CONICET of Argentina for financial support and to Ms Nancy Marcellini for technical assistance. Silvia L. Cuffini thanks ANCyT for the grant PICT 12–4927 (BID 802 OC/AR). The National Synchroton Light Source (NSLS), Brookhaven National Laboratory, Upton, NY, is supported by the United States Department of Energy (DOE), Division of Chemical Sciences and Division of Materials Sciences. The SUNY X3 beamline at the NSLS is supported by the Division of Basic Energy Sciences of the United States DOE.

REFERENCES

1. Figueroa JP. Report of the Workgroup on parasitic diseases. *Morb Mortal Wkly Rep.* 1999;48:118–125.

2. Ferreira RCC, Ferreira LCS. Mutagenicity of nifurtimox and benznidazole in the salmonella/microsome assay. *Braz J Med Biol Res.* 1986;19:19–25.

3. Radloff PD, Philips J, Nkeyi M, Hutchinson D, Krensner PG. Atovaquone and proguanil for *plasmodium falciparum* malaria. *Lancet.* 1996;347:1511–1514.

4. Li CJ, Li YZ, Pinto AV, Pardee AB. Potent inhibition of tumor survival in vivo by β-lapachone plus taxol: combining drugs imposes different artificial checkpoints. *Proc Natl Acad Sci USA.* 1999;96:13369–13374.

5. Sperandeo NR, Brun R. Synthesis and biological evaluation of pyrazolylnaphthoquinones as new potential antiprotozoal and cytotoxic agents. *ChemBioChem.* 2003;4:69–72.

6. Byrn SR, Pfeifer R, Stowell JF. *Solid-State Chemistry of Drugs*. 2nd ed. West Lafayette, IN: SSCI Inc; 1999.

7. Wells J. *Pharmaceutical Preformulation: The Physicochemical Properties of Drug Substances*. New York, NY: Ellis Horwood Ltd, John Wiley & Sons; 1993.

8. Brittain HG. *Physical Characterization of Pharmaceutical Solids* Vol 70. New York, NY: Marcel Dekker Inc; 1995.

9. Pagola S, Stephens PW, Bohle DS, Kosar AD, Madsen SK. The structure of malaria pigment β-haematin. *Nature.* 2000;404:307–310.

10. Spek AL. *PLATON, A Multipurpose Crystallographic Tool*. 2001. Utrecht, The Netherlands: Utrecht University. Available at: http://www.cryst.chem.uu.nl/platon/. Accessed: July 8, 2005.

11. Ghosh S, Ojala WH, Gleason WB, Grant DJW. Relationships between crystal structures, thermal properties and solvate stability of dialkylhydroxypyridones and their formic acid solvates. *J Pharm Sci.* 1995;84:1392–1399.

12. United States Pharmacopeial Convention. *United States Pharmacopeia XXVI.* Washington, DC:United States Pharmacopeial Convention Inc. 2003.

13. Dinnebier RE. GUFI Powder Diffraction Software. 2002. Available at: http://www.fkf.mpg.de/xray/html/body_gufi_software.html. Accessed: July 8, 2005.

14. Visser JW. A fully automatic program for finding the unit cell from powder data. *J Appl Cryst* [serial online]. 1969. Available at: http://sdpd.univ-lemans.fr/ftp/ito13.zip. Accessed: July 8, 2005.

15. Le Bail A, Duroy H, Fourquet JL. Ab-initio structure determination of $LiSbWO_6$ by X-ray powder diffraction. *Mat Res Bull.* 1988; 23:447–452.

16. Rodriguez-Carvajal J. FULLPROF: A program for Rietveld refinement and pattern matching analysis. *Abstracts of the Satellite Meeting on Powder Diffraction of the XV Congress of the IUCr.* 1990. Toulouse, France. Available at: http://www-llb.cea.fr/fullweb.powder.htm. Accessed: July 8, 2005.

17. Larson AC, Von Dreele RB. *GSAS, Generalized Crystal Structure Analysis System*. 1987. Los Alamos, NM: Los Alamos National Laboratory Report Number LA-UR-86-748. Available at: http://www.ccp14.ac.uk/ccp/ccp14/ftp-mirror/gsas/public/gsas/. Accessed: July 8, 2005.

18. Stephens PW, Pagola S. Powder Structure Solution Program *[computer program]. Version 2000.* Available at: http://powder.physics.sunysb.edu/programPSSP/pssp.html. Accessed: July 8, 2005.

19. Allen FH, Kennard O. 3D search and research using the Cambridge structural database. *Chem Design Automation News.* 1998;8:31–37.

20. Farrugia LJ. Program Ortep-3 for Windows. *J Appl Cryst* [serial online]. 1997. Available at: http://www.chem.gla.ac.uk/~louis/software/. Accessed: July 8, 2005.

21. Scott HG. The estimation of standard deviation in powder diffraction Rietveld refinements. *J Appl Crystallogr.* 1983;16:159–163.

22. Focés-Focés C, Llamas-Saiz AL, Claramunt RM, López C, Elguero JJ. Structure of 3(5)-methyl-4-nitropyrazole in the solid state: tautomerism, crystallography and the problem of desmotropy. *J Chem Soc Chem Commun.* 1994:1143–1145.

23. Fernández AE, de Bertorello MM, Manzo RH. Síntesis y propiedades espectroscópicas de aminoisoxazolilnaftoquinonas. *Anales Asoc Quím Argent.* 1982;70:49–60.

24. Sperandeo NR, de Bertorello MM, Briñón MC. Synthesis and some physicochemical properties of 2-hydroxy-N-(3,4-dimethyl-5-isoxazolyl)-1,4-naphthoquinone-4-imine derivatives. *J Pharm Sci.* 1994;83:332–335.

25. Dorn H, Zubek A. Bicyclische systeme aus acetessigester und 5-amino-1-methyl-,5-amno-1-benzyl- sowie 3(5)-aminopyrazol. *Chem Ber.* 1968;101:3265–3277.

26. Galwey AK. Thermal reaction of selected solids including reactants that melt during chemical change. *J Thermal Anal.* 1994;41:267–286.

27. Sperandeo NR, de Bertorello MM. Solid state characterization of new protozoocidal agents - aminoisoxazolylnaphthoquinones. *Thermochim Acta.* 2001;378:69–77.

28. Ford JL, Timmins P. *Pharmaceutical Thermal Analysis: Techniques and Applications*. New York, NY: Ellis Horwood Ltd, John Wiley & Sons; 1989.

29. Berbenni V, Marini A, Bruni G, Maggioni A, Riccardi R, Orlandi A. Physico-chemical characterization of different solid forms of spirono-lactona. *Thermochim Acta.* 1999;340-341:117–129.

30. Marel Van Der HW. Quantitative differential thermal analysis of clay mineral and other minerals. *Am Mineral.* 1956;41:222–224.

31. MacKenzie RC, Michell BD. Differential thermal analysis data: a review. *Analyst.* 1962;87:420–434.

32. Haleblian JK. Characterization of habits and crystalline modification of solids and their pharmaceutical applications. *J Pharm Sci.* 1975;64:1269–1288.

33. Tiwary AK, Panpalia GM. Influence of crystal habit on trimethoprim suspension formulation. *Pharm Res.* 1999;16:261–265.

34. Dresse A, Gegard MA, Lays A. Human pharmacokinetics of 2 crystalline and galenic forms of diflunisal, a new analgesic. *Pharm Acta Helv.* 1978;53:177–181.

35. Amidon GL, Lennernas H, Shah VP, Crison JR. A theoretical basis for a biopharmaceutic drug classification: the correlation of in vitro drug product dissolution and in vivo bioavailability. *Pharm Res.* 1995;12:413–420.